Nucleation and initial growth phase of diamond thin films on (100) silicon

X. Jiang, K. Schiffmann, and C.-P. Klages
Fraunhofer-Institut für Schicht- und Oberflächentechnik (FhG-IST), Bienroder Weg 54 E, D-38108 Braunschweig, Germany
(Received 6 January 1994; revised manuscript received 17 March 1994)

The nucleation of diamond on silicon (100) in a methane-in-hydrogen microwave plasma has been investigated by atomic-force microscopy, scanning electron microscopy, and reflection high-energy electron diffraction (RHEED). The nucleation of diamond was performed by application of an electrical substrate potential. It was found that three-dimensional nonfacetted islands are initially formed whose sizes increase with the deposition time. In spite of their very small sizes of a few nanometers, RHEED reveals that the islands are of crystalline-diamond structure. An induction time of about 6.5 min was necessary for the diamond nucleation, which is partly caused by the formation of a silicon-carbide surface layer due to the carbon diffusion into the substrates. The time dependence of nucleation density was investigated and fitted with a model kinetics, which considers the formation, destruction, and capture of active sites, germs, and nuclei. Analyses of the first-nearest-neighbor distance distributions reveal the formation of a depletion zone of nuclei around the existing islands. These results confirm the role of the adatom diffusion improved by the bias-enhanced ion bombardment. Analyses of the island-size and the island-height distributions show constant growth rate at the beginning of the diamond deposition. From the nearly constant ratios of the island height to island size, independent of the nucleation time, one can deduce that the thermodynamics accounts not only for the growth mode, but also for the island shape during deposition. The bias-enhanced ion bombardment during deposition may also increase the diffusion of the surface atoms of the islands, allowing the system to approach equilibrium.

I. INTRODUCTION

Due to its outstanding material properties, diamond is expected to become a very important material for applications ranging from tribological, optical, and thermal to active electronic applications.[1,2] With the development of various chemical-vapor-deposition (CVD) methods during the past few years economic preparation of synthetic diamond films became feasible.[2–5] The most crucial point to overcome for diamond applications, however, is the problem of achieving high-quality large area diamond films, i.e., the problem of heteroepitaxial diamond growth.[6] Therefore the study of diamond nucleation and growth is currently of great importance not only for basic investigations but also for the diamond film applications.[4,5,7] A fundamental understanding of the nucleation and growth mechanism of diamond crystals is essential to our ability to achieve high-quality heteroepitaxial diamond films.

The nucleation of diamond depends on the substrate material and is greatly affected by the process parameters applied for the deposition. In general, diamond nuclei grow very poorly on a mirror-polished silicon substrate due to the much higher surface energy of diamond relative to silicon [6 J/cm^2 for diamond, 1.5 J/cm^2 for silicon (111) plane],[1,8] and the relatively low sticking probability of the precursor for diamond nucleation. Therefore, an *ex situ* pretreatment of the substrate such as mechanical scratching with diamond powder,[9] ion implantation,[10] and production of defects and sharp edges on the substrate,[11] and predeposition of carbonaceous precursors or nondiamond carbon such as *a*-C:H or graphite[12,7] are commonly needed to obtain a continuous diamond film. These *ex situ* pretreatments, however, have so far caused only randomly oriented films.

It has been shown[13] that, in a physical-vapor-deposition (PVD) or a plasma-assisted chemical-vapor-deposition process, the film nucleation and growth is greatly influenced by the size, the ionization degree, and the energy distribution of the existing particles. Moreover, the properties of growing islands and films can also be affected by the substrate temperature, the gas pressure, and an extra bombardment with high-energy neutral particles or ions. This bombardment of neutral particles and ions during deposition causes similar effects to those provided by an increase in kinetic energy of the surface atoms of the deposits.

The application of a negative substrate potential is an effective way to increase the ionization degree and the energy of particles in the gas phase and therefore to realize the bombardment of the substrate surface. Previous investigations[14–17] have shown that applying a dc electric field to the substrate during diamond growth in a microwave plasma CVD process improves the nucleation and growth of diamond films. A positive substrate potential results in an improvement of the film quality.[16] For a predeposition process using a negative substrate bias voltage larger than -70 V and a relatively high methane concentration in the feed gas, an enormous enhancement of the generation of diamond nuclei on a silicon mirror surface was achieved.[14,15] Based on the film nucleation with help of a negative substrate potential, i.e., without the above described *ex situ* pretreatments, in the heteroepitaxial diamond growth on large-area β-SiC substrates has recently been achieved.[18] The heteroepitaxial

growth of diamond films on (100) silicon was reported at the DIAMOND'92 held in Heidelberg, Germany[19] (for more details see Ref. 20) using a similar technique. This success could be viewed as a significant step towards diamond microelectronic devices formed by single-crystalline diamond layers heteroepitaxially grown on silicon substrates. In contrast to the previous unsuccessful attempts of the heteroepitaxial growth on silicon the achievement is obviously based on the diamond nucleation without *ex situ* pretreatment of the silicon substrates. The mechanism of this kind of diamond nucleation is, however not well understood. Previous research using high-resolution cross-sectional transmission electron microscopy shows that a thin silicon carbide layer up to 10 nm and carbon clusters are formed before significant diamond nucleation occurs.[17] A similar suggestion was also made by Yugo, Kimurd, and Kandi.[21] Because the observed SiC interlayer and the carbon clusters are amorphous, only randomly oriented diamond crystals were grown. Monitoring of the stages of diamond nucleation using atomic force microscopy (AFM) and reflection high-energy electron diffraction (RHEED) has shown[22] that nonfacetted nuclei are initially formed which are of crystalline structure in spite of their very small sizes of a few nanometers. SiC of several monolayers was also detected on the silicon surface, however it is crystalline and epitaxially grown. It needs further investigations to decide whether the SiC phase is formed at the silicon and diamond interface, i.e., whether the diamond nuclei are grown on the thin epitaxial SiC surface layer or are in direct contact with the silicon substrates.

To improve the understanding of nucleation mechanism it is necessary to study the kinetics and energetics of the growth process. The generally accepted growth sequence in a vapor deposition process is adsorption, diffusion, and formation of clusters. Once such clusters are formed, they are likely to grow to larger islands, inhibiting nucleation in their immediate neighborhood[23] by acting as sinks for the diffusing adatoms. Such kinetic factors establish a correlation between the size and spatial distributions of the islands. Thermodynamics determines the growth mode if the process does not proceed too far from equilibrium: The surface atoms of an island will rearrange through diffusion to minimize the surface energy, i.e., the island shape is controlled by the energetics during growth.

Due to the difficulty of diamond nucleation (without substrate bias potential) and the fact that diamond is a metastable phase for most of the deposition processes used, i.e., the growth is far from thermodynamical equilibrium, only few investigations were performed. A kinetic approach was done recently, describing the nucleation of well separated particles on solid surfaces. A satisfactory agreement with experimental data was found.[24,25]

In this paper the initial development of diamond nuclei, formed in a microwave plasma on negatively biased single-crystalline (100) silicon substrates is observed. The dependencies of the nucleation density on the processing time are studied. Analyses of the island shape and of the first-nearest-neighbor distance distribution demonstrate that diamond island formation is driven by the energetics of the system whereas the nucleation rate, the island-side distribution, and the formation of depletion zones around the islands are affected by the growth kinetics.

II. EXPERIMENT

A. Formation of the diamond islands

1×2 cm^2 *n*-type (100) silicon wafers were used as substrates. The wafers were chemically cleaned with acetone in an ultrasonic bath for 10 min and mounted in a stainless-steel ASTEX reactor.[15] After pumping the chamber to a pressure of about 10^{-3} mbar the substrates were etched *in situ* in a hydrogen microwave plasma for 20 min to remove the native surface oxide layer. Diamond nuclei were then formed in a 1% methane-in-hydrogen microwave plasma. The diamond growth in a microwave plasma CVD process, like other plasma-assisted methods depends in a very complex way on the preparation conditions. Because many parameters are coupled with each other, the optimization is not always easy. The deposition parameters given in Table I were selected after a systematic search for the optimal growth conditions: The applied input microwave power was 900 W. The wafers were inductively heated to a temperature around 850 °C. The substrates were dc-biased at −150 V relative to the vacuum chamber which was electrically grounded.

B. Characterization of the deposits

After deposition the samples were immediately brought into an UHV chamber. The reflection high-energy electron diffraction (RHEED) was then performed to monitor the crystallographic properties of the deposits.

A commercial, ambient atomic force microscope, which has outstanding possibilities in film analysis and can provide "atomic resolution" images of CVD diamond flat surfaces,[26] was employed for characterizing the morphology of the nuclei. A crucial point for imaging small particles using the atomic-force-microscope is the shape of the force sensor tip which can lead to image artifacts if

TABLE I. Preparation conditions of the specimens.

Process	H_2 (vol. %)	CH_4 (vol. %)	Gas pressure (mbar)	Temperature (°C)	Bias voltage (V)	Power (W)
Plasma etching[a]	100	0	20	850	−150	900
Nucleation[a]	99	1	20	850	−150	900

[a]Plasma etching for cleaning the substrates lasts 20 min; the nucleation times for different samples are 0, 2.5, 5, 7.5, 10, 12, 15 min, respectively.

the particle dimensions are comparable or smaller than that of the tip apex. Assuming a tip with radius of curvature of R_{tip} and a half sphere particle with radius of curvature R_{part}, the apparent particle height in the atomic force microscope image is then correctly given by $H = R_{part}$ while its lateral size (diameter) is enlarged to[27]

$$D = 2R_{part}\sqrt{1+2(R_{tip}/R_{part})} .$$

In our atomic force microscope experiments we used conventional pyramidal Si_3N_4 tips with a radius of curvature of about 50 nm, which is in most cases much larger than typical nucleus sizes. We therefore used the atomic force microscope only for determination of nucleus height distributions, while nucleus sizes were investigated by a JSM 6300F field emission scanning electron microscope (SEM) with a lateral resolution of 2–3 nm.

III. RESULT AND DISCUSSION

A. Observation and crystallographic properties of the nuclei

To study the early growth stage of epitaxial diamond films on (100) silicon a series of samples was grown with interruptions at 2–3 min intervals and observed by an atomic force microscope and a scanning electron microscope. Figure 1 shows 1.5×1.5 μm^2 atomic force microscope images taken from samples after 7.5, 10, 12, and 15 min depositions, respectively, on silicon (100). The bright protrusions in the images correspond to diamond islands. From the atomic force micrographs of the samples prepared with deposition time less than 6.5 min no islands can be found. For a deposition time of 7.5 min [Fig. 1(a)] islands of several nanometers in height were formed. The islands shown in Figs. 1(a)–(d) are stable, as confirmed by the further diamond growth. The island size and the island density increase with the deposition time and the amount of material deposited. After 15 min deposition [Fig. 1(d)] the major part of the surface was covered with the islands. The islands are, however, still separated from each other, as observed by scanning electron microscopy. The "appearance" of the island coalescence in Fig. 1(d) is due to the tip artifacts of the atomic force microscope.

The crystallographic properties of the nuclei were investigated by means of reflection high-energy electron diffraction, indicating the crystalline diamond structure of the islands in spite of their very small size of several nanometers. The RHEED patterns obtained from the specimens with a deposition time less than 6.5 min show only spots due to diffraction by epitaxial cubic SiC of several monolayers. Diffraction from diamond is not detectable for the samples with a deposition time less than 6.5 min, confirming the results obtained by AFM. With a deposition time greater than 6.5 min diffraction of diamond nuclei appears and the intensity increases with increasing deposition time, whereas the intensity of diffraction from the substrate surface decreases.

The fact that the diamond nuclei are not formed for a deposition time less than 6.5 min could be interpreted partly in terms of carbon diffusion into the silicon substrate which controls the steady-state carbon supersa-

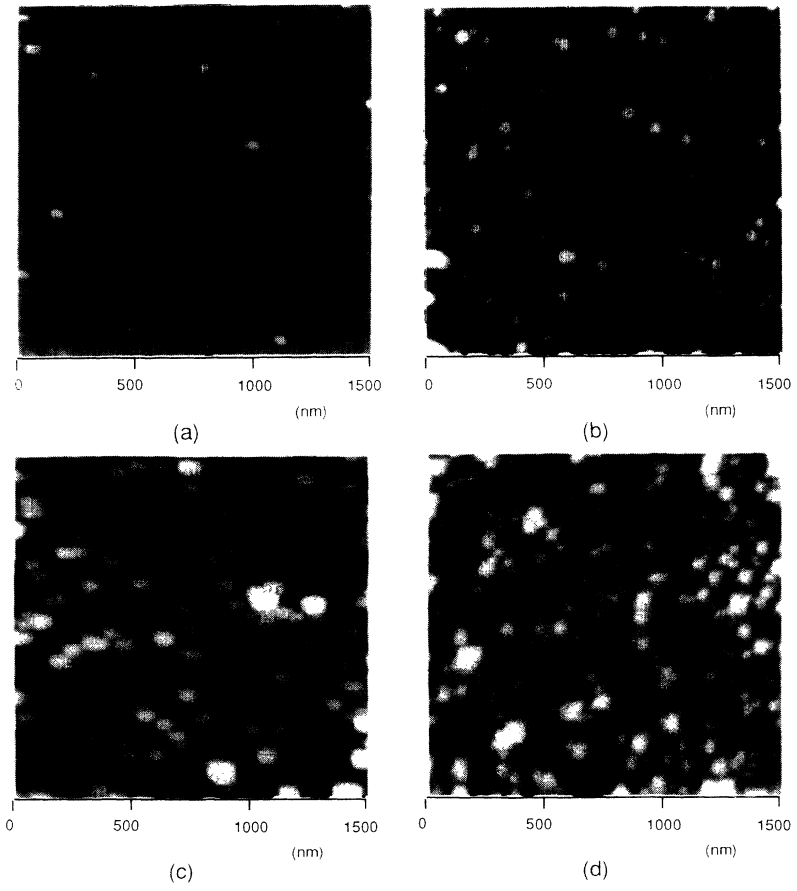

FIG. 1. 1500×1500 nm^2 micrographs of atomic force microscopy showing the surface morphologies after (a) 7.5, (b) 10, (c) 12, and (d) 15 min depositions.

turation at the surface during deposition. Silicon substrates can absorb carbon into the bulk by forming carbide and thereby delay the diamond nucleation. Diamond deposition on other kind of substrates has indicated that the induction times for nucleation are long for substrates with high carbon diffusion rates (Ti, Nb, Mo).[28]

Following diamond CVD growth on silicon, an SiC interlayer was often detected.[29,30] It was found that the SiC layer thickness decreases as the initial methane to hydrogen ratio in the methane-in-hydrogen gas mixture used for deposition increases from 0.3% to 1% and the SiC layer could not be detected in samples deposited at 2% methane in hydrogen. The SiC layer thickness was 40–70 Å for microwave plasma growth at 0.5% methane in hydrogen.

Although SiC is detected at the diamond-silicon growth interface, a SiC layer deposited on silicon resulted in no nucleation enhancement. The final SiC layer thickness is achieved in a very short time (only about 2 min),[31] however the diamond nucleation occurs later (6.5 min in this study), which indicates that the delay caused by the carbide formation is not equal to the whole induction time of nucleation. On the other hand, this fact indicates also that the carbide formation is not a necessary condition for subsequent diamond growth, but a competitive carbon reaction channel.[32]

B. Time dependence of nucleation density: Agreement with the kinetics

By means of scanning electron microscopy the dependences of island-density and island-size distribution of the specimens on the deposition time were analyzed. The nucleation density N (islands/cm^2) is plotted in Fig. 2 as a function of nucleation time t, which is counted from the induction time t_{ind}. t_{ind} is generally defined as a time when the aggregates formed initially have grown to a diameter which is detectable in the electron microscope.[33]

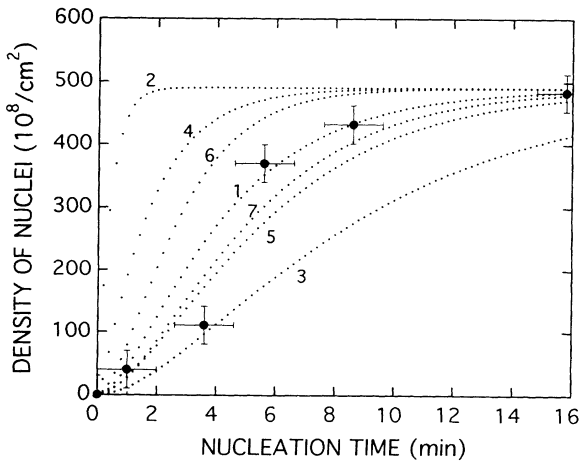

FIG. 2. Nucleation density (islands/cm^2) as a function of processing time. In the abscissa a induction time of 6.5 min is subtracted. The curves are obtained by computer modeling using Eq. (1) and different values of α and β: (1) $\alpha=0.014\,26$ and $\beta=0.005$; (2) $\alpha=1$ and $\beta=0.04$; (3) $\alpha=0.006$ and $\beta=0.0025$; (4) $\alpha=0.1$ and $\beta=0.01$; (5) $\alpha=0.008$ and $\beta=0.04$; (6) $\alpha=0.014\,26$ and $\beta=0.01$; (7) $\alpha=0.08$ and $\beta=0.005$.

According to the results obtained by AFM and RHEED the induction time in this study is about 6.5 min. In Fig. 2 it is evident that, once the nucleation begins, the nucleation density increases rapidly to 4.3×10^{10} cm^{-2} within 8.5 min. The main part of the substrate surface is then covered by the nuclei and the increase of the density, i.e., the nucleation rate is lowered with increasing coverage. It was found that, under the conditions applied in this study, the whole substrate surface is covered by the diamond nuclei after about 25 min deposition and a continuous film is formed.

In what follows we will try to make a kinetic approach to the nucleation data by a model established recently by Tomellini, Pollini, and Sessa[24] in order to provide a definite framework at a molecular scale. The proposed model kinetics predicts the time evolution of active sites, germs, and nuclei of the substrate surface and includes the capture of germs and active sites at the borders of the growing diamond phase. By solving three differential equations, written in terms of the surface densities of active sites, germs, and nuclei one obtains the nucleation density $N(t)$ of well separated islands at the solid surfaces,

$$N(t)=N_\infty[1+\beta(\alpha-\beta)^{-1}\exp(-\alpha t) -\alpha(\alpha-\beta)^{-1}\exp(-\beta t)] , \quad (1)$$

$$\alpha+\beta=n_f+k_c+k+n_d , \quad (2)$$

$$\alpha\beta=kn_f+kk_c+n_dk_c , \quad (3)$$

where N_∞ is the limiting value of the surface densities of the nuclei N when $t\to\infty$ and n_f, k_c, k, and n_d are the probabilities, per unit time, of the occurrence of the corresponding kinetic steps. In fact the N_∞ is the density of the nuclei when the whole substrate surface is covered. In this research the N_∞ is approximately 4.9×10^{10}/cm^2. Using Eq. (1) a fitting of the experimental data was performed by adjusting the parameters α and β. Figure 2 gives the time dependences of the nucleation density calculated with different values of α and β. By a careful selection of α and β, e.g., $\alpha=0.014\,26$, and $\beta=0.005$, four of the experimental data can be fitted by the computer modeling, indicating that the kinetic model of *active sites–germs–nuclei* sequence may be applicable for the bias-enhanced nucleation conditions. The poor fit of the data point at 3.5 min is possibly caused by the irreproducible plasma conditions. In general, the observed behavior of α and β should reflect the dependence of the rate constants for germ formation from an active site n_f and for nucleus formation from a germ k, on substrate temperature and gas composition.[25] Since the α/β ratio derived from the fit in Fig. 2 is 2.84 the rate constant of active site formation from a germ n_d is then smaller than that of germ formation from a active site n_f under present deposition conditions.

C. First-nearest-neighbor-distance distribution

It has been shown in this work that kinetics is largely responsible for the observations related to the nucleation rate. In addition, the growth kinetics also determines the distance between the nearest-neighbor nuclei, an effect

demonstrated by the formation of depletion zones around the islands. Due to surface diffusion the adatom concentration depends on the distance from the islands because the islands represent a sink for adatoms.[23]

The theoretical distribution of first-nearest neighbors $W(r)$ when the nuclei are dispersed randomly on the support may be derived from the calculations established. If ρ is the number density of crystallites dispersed randomly, the probability of not finding crystallites on a surface S follows a Poisson distribution $W_1=\exp(-\rho S)$. The probability of finding a crystallite on a surface element dS is given by $dW_2=\rho dS$. Thus the probability of not finding a crystallite in S but finding one in dS is $dW=W_1 dW_2=\rho\exp(-\rho S)dS$. This relation may be applied to the problem directly. Indeed, the nearest neighbor is defined by the fact that there is no crystallite at a distance r from a crystallite taken as origin, and at a distance between r and $r+dr$ one notes the presence of a crystallite which is the first nearest neighbor

$$dW_{\text{random}}(r,dr)=2\pi\rho r\exp(-\pi\rho r^2)dr = W_{\text{random}}(r)dr\ . \quad (4)$$

From the AFM/SEM images, we can measure the distribution

$$W_{\text{measured}}(r)=\rho(r,dr)/N\ , \quad (5)$$

where $\rho(r,dr)$ is the number of islands with nearest-neighbor distance between r and $r+dr$ and N is the total number of islands counted. Such measurements have been performed by Schmeisser and co-workers[34,35] for an evaporated Au/NaCl system and by Yang, Yuo, and Weaver[36] for an evaporated Ge/GaAs system. Figures 3(a) and (b) compare the distributions measured $W_{\text{measured}}(r)$ with the distributions of the first nearest neighbor corresponding to a random distribution $W_{\text{random}}(r)$ for diamond nuclei depositions of 10 and 12 min, respectively, showing that the measured distributions are shifted to larger distances, as expected if there is a depletion zone around each cluster. The measured distributions are narrower than the random distributions and the width decreases with increasing deposition time. The enlargement of the distance between neighboring clusters compared to a random distribution has previously been explained in terms of cluster-cluster interactions, i.e., an interaction of neighboring clusters due to lattice distortion of the substrate surface between the clusters.[37] For a random distribution, the nucleation of a given cluster is independent of all others. For the diamond island growth the enlargement of nearest-neighbor distance implies that the diamond nucleation is strongly influenced by the existing nuclei—a repulsive interaction among the clusters exists and the clusters tend to separate. The cluster-cluster interaction model is normally based on the fact that the existing nuclei move during the process. Considering the strong covalent bonding in the diamond to silicon system, the movement of a diamond nucleus on silicon seems to be difficult. In this case the factor of surface diffusion of the adatoms must also be taken into account.

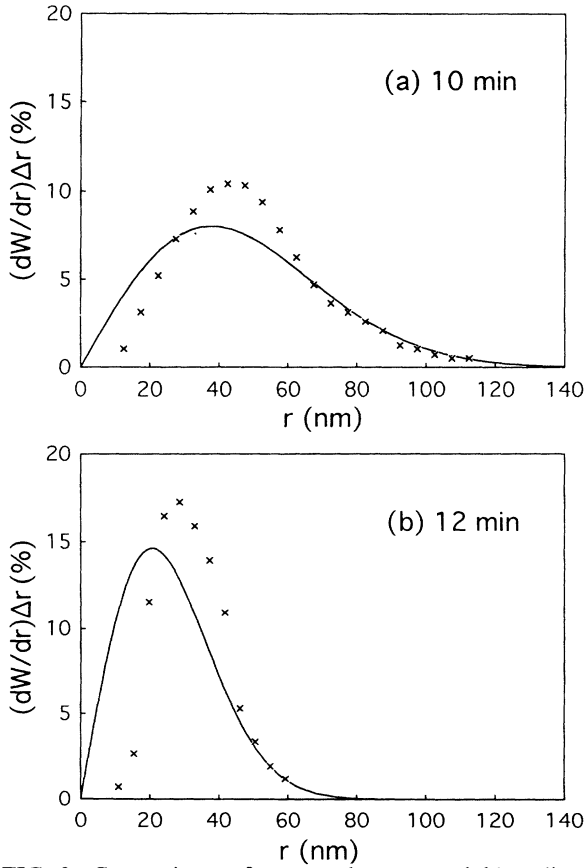

FIG. 3. Comparisons of measured nearest-neighbor distance distributions and the distributions predicted from a random nucleation model for (a) 10 min and (b) 12 min depositions.

The process on a substrate surface in the initial stage of growth may be described by the following sequence: (a) vapor species arrive on the substrate surface (atoms, molecules, and/or radicals) and are adsorbed; (b) the adatoms diffuse over the substrate surface and a part of the adatoms desorbs from the surface into the vacuum; (c) the adatoms combine and form clusters due to fluctuations of the local adatom concentration; (d) nuclei grow by capture of the adatoms or by direct impingement of the atoms from vapor phase. Adsorbed species diffuse on the substrate surface until they meet each other and form clusters. Once such nucleation centers are established, they are likely to grow to larger islands, inhibiting additional nucleation in their immediate neighborhood by acting as sinks for the diffusing atoms. A schematic diagram concerning the adatom concentration is given in Fig. 4. The adatom concentration decreases to zero on

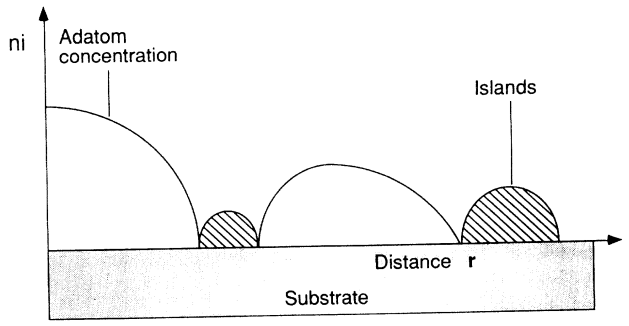

FIG. 4. Schematic diagram of adatom concentration around islands on the substrate surface.

the border of one island. From Fig. 3 we obtain a depletion zone for nucleation in the range of about 10 nm. This value should correspond to the minimum distance from a nucleus where the adatom concentration is influenced by the existing nucleus.

As mentioned above, the enlargement of the first nearest-neighbor distance provides a strong evidence for the adatom diffusion. Due to the increased ion bombardment by application of the negative bias voltage at a temperature $T_s > 800\,^{\circ}\mathrm{C}$ the adatom diffusion will be enhanced, which could be the key for the diamond nucleation. The nucleation of diamond depends strongly on the substrate material and is greatly affected by the initial surface conditions of the substrate. Due to the very high surface energy of diamond (≈ 6 J/cm^2) (Ref. 1) and the reactively low sticking probability and low mobility of the precursors for diamond nucleation, diamond nuclei grow very poorly on a mirror polished silicon substrate under conventional experimental conditions. Applying a negative substrate potential can, however, increase the bombardment of positively charged energetic ions and the mobility of the adatoms. The surface diffusion of the adsorbed precursors increases. This favors the probability of the adatoms meeting each other and forming clusters. Certainly there are also some other factors of applying a substrate bias voltage which could influence the nucleation, for example, the interruption of the Si-H or C-H bonding which may lead to an increase of the sticking coefficient of carbon atoms and the attraction of the positively charged hydrocarbon species, which leads to a carbon supersaturation at the substrate surface.

The competition between growth and nucleation of new clusters depends on the adatom concentration and is therefore dependent on the distance r from the islands. In the kinetic theory the adatom concentration can be calculated from differential equations, which contain the diffusion rate, the arrival rate, the desorption rate and in second approximation also the capture rate. Such kinetic factors establish a correlation between nearest-neighbor distance distribution and the size distribution of the islands.

D. Island-size and island-height distributions

The condensation of the gas phase species onto a substrate to form islands involves both kinetic processes and thermodynamic factors. The importance of thermodynamics is widely recognized as far as its influence on growth modes is concerned. The energetics of the system are however also important in determining the shape of the islands because the overlayer atoms will rearrange to form crystallites to minimize the system free energy. Thus by analyzing the shape of the islands, we demonstrate the energetics during growth.

Figure 5 shows the histograms of the island sizes for the nucleation and initial growth stage, as derived from the SEM pictures of the samples after deposition times of 7.5, 10, 12, and 15 min, respectively. The histogram in Fig. 5(a) is relatively narrow and it reaches a maximum at an island size of 45 Å. For 10 min deposition, the distribution width increases and the peak shifts to 75 Å [Fig. 5(b)]. After 12 min deposition the island sizes become much larger as is reflected in the size distribution of Fig. 5(c). The distribution width increases strongly and the peak maximum has increased to 225 Å. The change of the island size distribution shapes for diamond deposition of various times are very different from the nucleation of metal films in PVD processes.[35] In the case of metal-film deposition, the left branch of the distribution of the nuclei drops below the previous measured values, i.e., in later stages of deposition the population of small clusters is smaller than the population of clusters of same size at earlier times. In the main part of distribution, on the other hand, the distribution ranges do not extend so far as in the case of diamond deposition. The distribution difference between depositions of metal and diamond films might be interpreted in terms of the different mobilities of diamond and metal clusters. Due to the strong covalent bonding of the interface between diamond and substrates, the mobility of diamond clusters is low and a capture of the nuclei is difficult. While the nuclei grow, new clusters will continuously be formed on the uncovered area beyond the depletion zone described previously and grow larger, resulting in an increase of island density and an extended nucleus size distribution. The maximum of the distribution moves to a larger size due

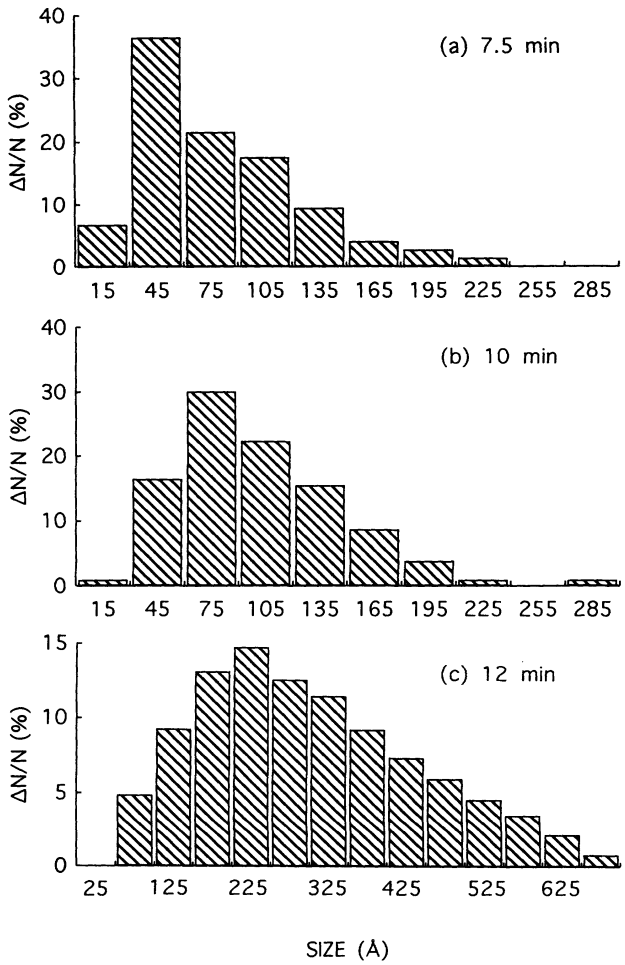

FIG. 5. Histograms of the islands sizes, as derived from the scanning electron micrographs for (a) 7.5 min, (b) 10 min, and (c) 12 min depositions.

to the crystal growth. In contrast, the mobility of the metal clusters is relatively high.[38] The small clusters, which have higher mobilities than larger ones, will often be captured by another one. So the density of small clusters is lower than that of same size at earlier time. The maximum of the size distribution moves also to a larger size, however the shape of the size distribution remains.

From the island-size distributions at different deposition times, one can obtain the relationship between the maximum island sizes and the deposition times and the growth rate of initial islands. Figure 6 shows the time dependence of the maximum island size. From the nearly linear dependence a initial growth rate of 0.63 μm/h is calculated.

To examine the island shape, we measured the island-height distributions on the same specimens used for the island-size measurements, i.e., for deposition of 7.5, 10, and 12 min, respectively. Atomic force microscopy was applied for the measurements. In Fig. 7 the histograms of the island height are plotted for different deposition times as a function of the island height. It is again evident that, besides the shifting of the maximum due to the island growth the distribution extends over a large range as deposition time is increased. The time dependence of the maximum island height is also obtained from Fig. 7 and shown in Fig. 6. The island-height distributions are very similar to the island-size distributions. Statistical AFM study of different islands shows a proportionality of the island height to island size. The identical distributions in Figs. 5 and 7 indicate that, for all the samples, the ratios of the island height-to-size approach a constant with an average value of about 1, nearly independent of island size.

The independence of the island height-to-size ratios offers us an evidence of surface energy minimizing of the islands during deposition and furthermore demonstrates that the diamond island shapes are indeed controlled by the energetics of the system. As already mentioned at the beginning of this section, the energetics determines the growth mode of a film. Depending principally on surface free energies for the substrate and the overlayer, σ_s and σ_f, and the interfacial free energy σ_i, three different modes of film growth can be distinguished:[37] (i) Volmer-Weber (VW, $\sigma_s < \sigma_f + \sigma_i$), three-dimensional (3D) island growth; (ii) Frank–van der Merwe (FM, $\sigma_s > \sigma_f + \sigma_i$), layer-by-layer growth; and (iii) Stranski-Krastanov (SK), 3D islands on top of one or a few epitaxial layers. For low strain energy in the films, FM growth typically occurs for overlays with low surface energy relative to the substrate, whereas VW growth is typical for those with high surface free energy. The much higher surface energy of diamond relative to silicon leads to the 3D island (VW) growth of diamond on silicon.

Once the VW growth of a film is established, the island shape will furthermore be influenced by the energetics. For small sizes (less than 30 Å) the islands generally show no faceting. Their contours appear to be quasihemispherical. For islands with sizes greater than 30 Å their forms are distinguished as equilibrium and kinetic form.

The real equilibrium forms of 3D crystallites may be obtained under particular experimental conditions. The

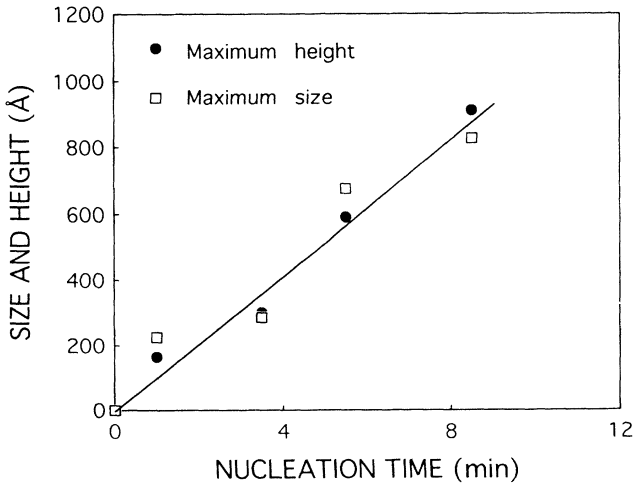

FIG. 6. Maximum island size and maximum island height as a function of the nucleation time, i.e., the depoisition time −6.5 min.

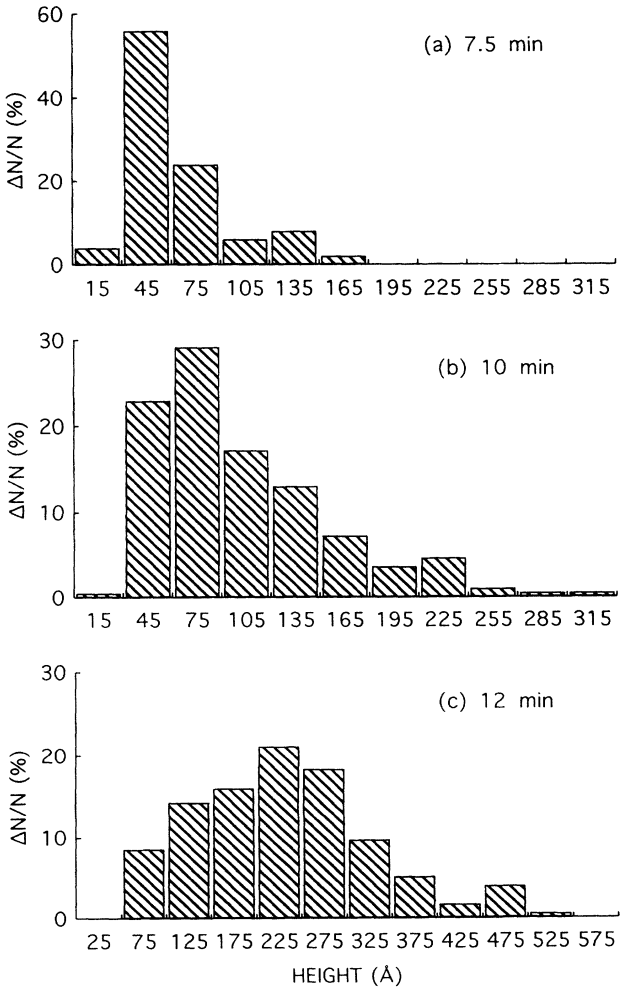

FIG. 7. Histograms of the island heights, as derived from the AFM images for (a) 7.5 min, (b) 10 min, and (c) 12 min depositions.

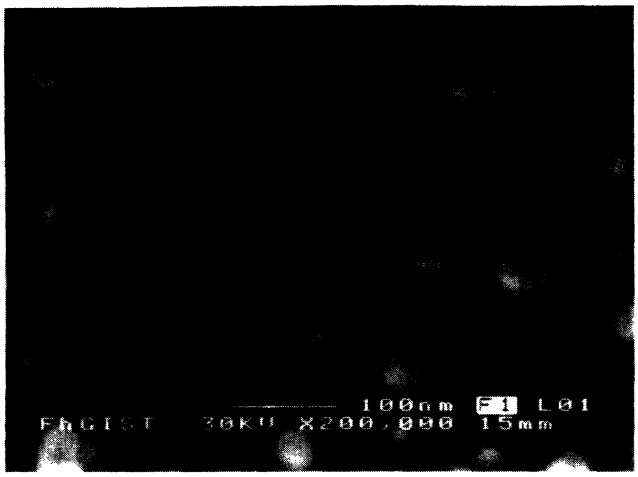

(a)

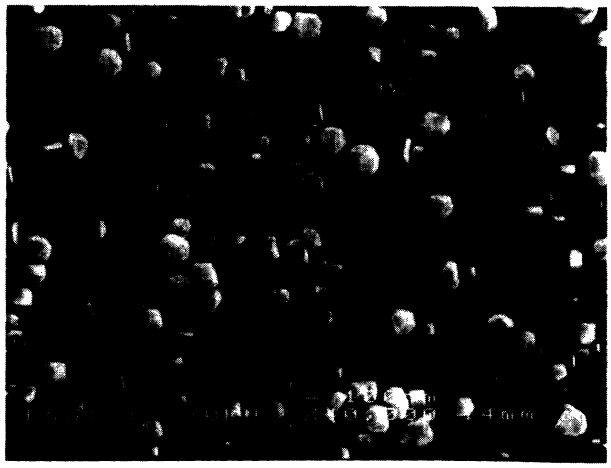

(b)

FIG. 8. (a) SEM image of the islands after 12 min depositon under substrate bias condition. (b) SEM photograph of a sample deposited on a grounded substrate for 30 min after 7 min bias nucleation, using 0.5 vol. % methane.

following two ways are often used: (a) increasing the incident flux of the species in the gas phase. The crystallites receive the species that migrate on the substrate and the crystallite. It takes place at a moderate temperature if the activation energy of diffusion is low; (b) without incident flux. It is only possible when the activation barrier of formation of an adatom is overcome and the adatoms may diffuse on the crystallite and join a favorable site which modifies the island form. In many experiments it is observed that, once kinetic forms are obtained, an attempt may be made to transform them into equilibrium forms by thermal annealing. However, the temperature to do this is generally high.

Concerning the CVD diamond growth in our experiments both above described factors are recognizable. For the bias nucleation, a relatively high methane concentration was applied. The attraction of the positively charged carbon containing species may produce a carbon supersaturation at the substrate surface. In addition the negative electrical potential of the substrate accelerates the ion towards the substrate, realizing a high ionization degree of the species and the ion bombardment of the existing islands. The ion bombardment during deposition causes a kinetic energy increase of the surface atoms, which often plays a similar role as thermal annealing.

Figure 8 shows a SEM photograph, obtained from a sample after 12 min bias nucleation, which confirms the quasihemispherical forms of the islands. If we turn off the substrate bias voltage and decrease the methane concentration the diamond crystallites will then grow under a kinetics dominated condition and the kinetical forms of the crystallites will be achieved. Figure 8(b) represents a sample, which was deposited without bias voltage with 0.5% methane concentration for 30 min after 7 min bias nucleation.

In summary, the results demonstrate that the island formation and island shapes are indeed controlled by process thermodynamics. The increased ion bombardment due to the negative substrate bias potential enhances the self-diffusion of the surface atoms of the nuclei and could allow the system to approach equilibrium. The selective nucleation, which has been recently achieved,[39,40] demonstrates the importance of surface ion bombardment.

IV. SUMMARY

The initial development of diamond nucleation and growth on silicon (100) was monitored using atomic force microscopy, scanning electron microscopy, and reflection high-energy electron diffraction. The destination of this work is to distinguish the effect of kinetics and energetics and to understand the role of substrate bias voltage during an early stage of the diamond nucleation and growth process. It has been found that, on a biased (100) silicon in a microwave plasma at 700–900 °C, three-dimensional nonfacetted islands are initially formed whose size increases with deposition time. There is an induction time of about 6.5 min for the diamond nucleation, which is probably caused in part by the formation of an SiC carbide surface layer. We have demonstrated first-nearest-neighbor-distance distribution, showing an enlargement of the first-nearest-neighbor distance. This discovery, together with the analysis of the island-size and the island-height distributions, reveals clearly the improvement of the surface diffusion of the adatoms most probably due to the increased ion bombardment.

ACKNOWLEDGMENTS

The work was financially supported by BMFT under Grant No. 03M2727B4 and by Daimler Benz AG. The RHEED study was performed by A. Westphal.

[1]*The Properties of Diamond,* edited by J. E. Field (Academic, London, 1979).
[2]K. E. Spear, J. Am. Ceram. Soc. **72**, 171 (1989).
[3]J. C. Angus and C. C. Haymann, Science **241**, 913 (1988).
[4]W. A. Yarbrough and R. Messier, Science **39**, 1 (1989).
[5]F. G. Celii and J. E. Butler, Annu. Rev. Phys. Chem. **42**, 643 (1991).
[6]A. Collins, Semicond. Sci. Technol. **4**, 605 (1989).
[7]J. C. Angus, Z. Li, M. Sunkara, R. Gat, A. B. Anderson, S. P. Mehandru, and M. W. Geis, in *Proceedings of the Second International Symposium on Diamond Materials,* edited by A. J. Purdes *et al.* (The Electrochemical Society, Pennington, NJ, 1991), p. 125.
[8]K. Ishibashi and S. Furukawa, Jpn. J. Appl. Phys. **24**, 912 (1985).
[9]P. K. Bachmann, W. Drawl, D. Knight, R. Weimer, and R. F. Messier, in *Diamond and Diamond-like Material Synthesis,* edited by G. H. Johnson, A. R. Badzian, and M. W. Geis (Materials Research Society, Pittsburgh, 1988), p. 99.
[10]S. J. Lin, S. L. Lee, J. Hwang, and T. S. Lin, J. Electrochem. Soc. **139**, 3255 (1992).
[11]P. A. Dennig and D. A. Stevenson, Appl. Phys. Lett. **59**, 1562 (1991).
[12]A. A. Morrish and P. E. Pehrsson, Appl. Phys. Lett. **59**, 417 (1991).
[13]K. Reichelt and X. Jiang, Thin Solid Films **191**, 91 (1990).
[14]S. Yugo, T. Kanai, T. Kimura, and T. Muto, Appl. Phys. Lett. **58**, 1036 (1991).
[15]X. Jiang, C.-P. Klages, R. Zachai, M. Hartweg, and H.-J. Füβer, Proceedings of Diamond '92, Heidelberg, 1992 [Diamond Rel. Mater. **2**, 407 (1993)].
[16]S. Yugo, T. Kimura, and T. Muto, Vacuum **41**, 1364 (1990).
[17]B. R. Stoner, G.-H. Ma, S. D. Wolter, and J. T. Glass, Phys. Rev. B **45**, 11 067 (1992).
[18]B. R. Stoner and J. T. Glass, Appl. Phys. Lett. **60**, 698 (1992).
[19]X. Jiang and C.-P. Klages, Proceedings of Diamond '92, Heidelberg, 1992 [Diamond Rel. Mater. **2**, 1112 (1993)].
[20]X. Jiang, C.-P. Klages, R. Zachai, M. Hartweg, and H.-J. Füβer, Appl. Phys. Lett. **62**, 3428 (1993).
[21]S. Yugo, T. Kimura, and T. Kanai, Proceedings of Diamond '92, Heidelberg, 1992 [Diamond Rel. Mater. **2**, 328 (1993)].
[22]X. Jiang, K. Schiffmann, A. Westphal, and C.-P. Klages, Appl. Phys. Lett. **63**, 1203 (1993).
[23]R. Kern, G. Le Lay, and J. J. Metois, in *Current Topics in Materials Science,* edited by E. Kaldis (North-Holland, Amsterdam, 1979), Vol. 3, p. 131.
[24]M. Tomellini, R. Polini, and V. Sessa, J. Appl. Phys. **70**, 7573 (1991).
[25]E. Molinari, R. Poloni, V. Sessa, M. L. Terranova, and M. Tomellini, J. Mater. Res. **8**, 785 (1993).
[26]V. Baranauskas, M. Fukui, C. R. Rodrigues, N. Parizotto, and V. J. Trava-Airoldi, Appl. Phys. Lett. **60**, 1567 (1992).
[27]Calculated under assumption of spherical forms of the islands and the force sensor tips.
[28]P.-O. Joffreau, R. Haubner, and B. Lux, Int. J. Refract Hard Metals **7**, 186 (1988).
[29]B. E. Williams and J. T. Glass, J. Mater. Res. **4**, 373 (1989).
[30]R. Meilunas, M. S. Wong, K. C. Sheng, R. P. H. Chang, and R. P. Van Duyne, Appl. Phys. Lett. **54**, 2204 (1989).
[31]R. W. Collins, Y. Cong, Y.-T. Kim, K. Vedam, and Y. Liou, Thin Solid Films **181**, 565 (1989).
[32]F. G. Celii and J. E. Butler, Ann. Rev. Phys. Chem. **42**, 643 (1991).
[33]M. Harsdorff and W. Jark, Thin Solid Films **128**, 79 (1985).
[34]H. Schmeisser and M. Harsdorff, Philos. Mag. **27**, 739 (1973).
[35]H. Schmeisser, Thin Solid Films **22**, 83 (1974).
[36]Y.-N. Yang, Y. S. Luo, and J. H. Weaver, Phys. Rev. B **46**, 15 387 (1992).
[37]K. Reichelt, Vacuum **38**, 1083 (1988).
[38]J. J. Metois, K. Heinemann, and H. Poppa, Philos. Mag. **35**, 1413 (1977).
[39]S. Katsumata and S. Yugo, Diamond Rel. Mater. **2**, 1490 (1993).
[40]X. Jiang, E. Boettger, M. Paul, and C.-P. Klages, Appl. Phys. Lett. (to be published).

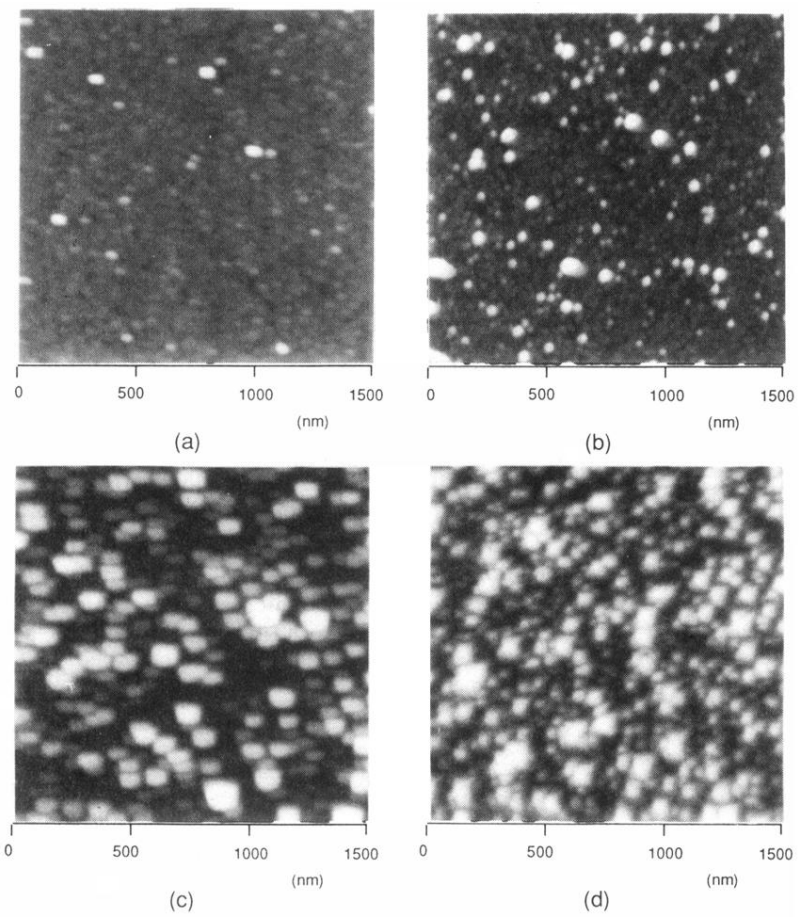

FIG. 1. 1500×1500 nm^2 micrographs of atomic force microscopy showing the surface morphologies after (a) 7.5, (b) 10, (c) 12, and (d) 15 min depositions.

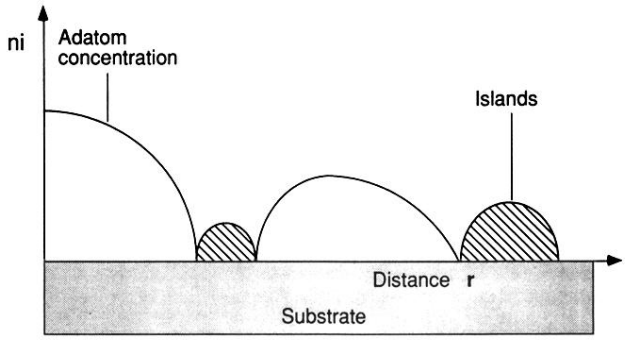

FIG. 4. Schematic diagram of adatom concentration around islands on the substrate surface.

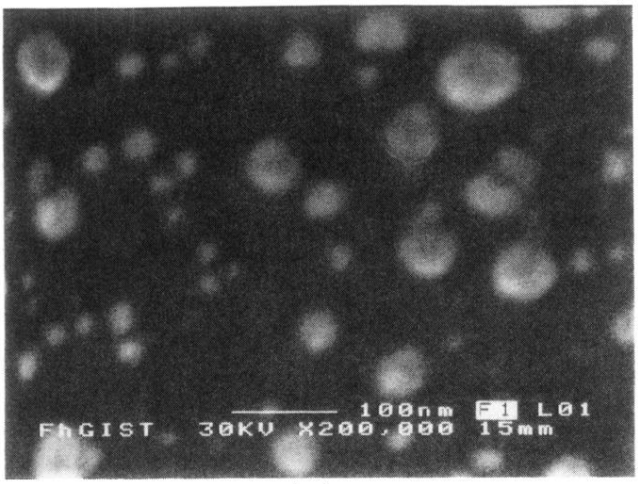

(a)

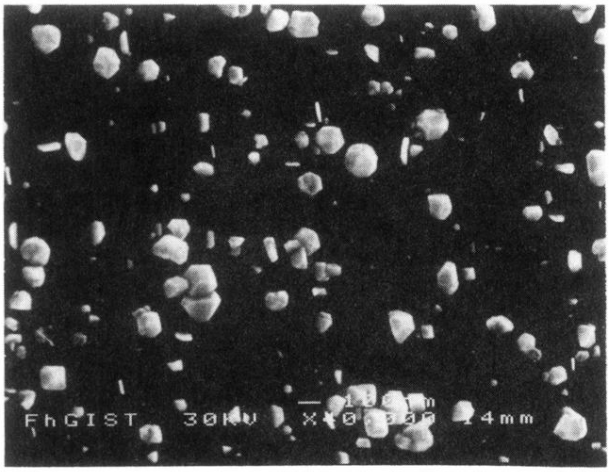

(b)

FIG. 8. (a) SEM image of the islands after 12 min depositon under substrate bias condition. (b) SEM photograph of a sample deposited on a grounded substrate for 30 min after 7 min bias nucleation, using 0.5 vol. % methane.